RESEARCH ARTICLE

Shallow roots of different crops have greater water uptake rates per unit length than deep roots in well-watered soil

Yannik Müllers · Johannes A. Postma · Hendrik Poorter · Johannes Kochs ·
Daniel Pflugfelder · Ulrich Schurr · Dagmar van Dusschoten

Abstract

Purpose Commonly, root length distributions are used as a first approximation of root water uptake profiles. In this study we want to test the underlying hypothesis of a constant water uptake rate per unit root length over depth.

Methods Root water uptake profiles were measured using a novel sensor technology. Root length was measured with MRI and by scanning harvested roots. Experiments were performed with pot-grown barley (*Hordeum vulgare*), maize (*Zea mays*), faba bean (*Vicia faba*), and zucchini (*Cucurbita pepo*).

Results For barley, maize, and faba bean, we found that roots in the top 15 cm had significantly greater water uptake rates per unit length than roots in the bottom 30 cm. For zucchini, the trend was similar but not significant. Therefore, variation of root water uptake rates with depth could be explained only partly (61–71%) by a variation of root length with depth.

Conclusion The common approximation of root water uptake profiles by root length distributions relies on constant water uptake rates per unit root length. This hypothesis does not hold in our study, as we found significantly greater water uptake rates per unit length in shallower than in deeper roots. This trend was consistent among species, despite the partly strong variation in physiological parameters. We suggest that this is caused by a decreasing axial transport conductance with depth. This might result in a general underestimation of water uptake rates in shallow soil layers when they are approximated by the root length distribution.

Responsible Editor: Hans Lambers.

Y. Müllers · J. A. Postma · H. Poorter · J. Kochs ·
D. Pflugfelder · U. Schurr · D. van Dusschoten (✉)
Plant Sciences, IBG-2, Forschungszentrum Jülich, Jülich, Germany
e-mail: d.van.dusschoten@fz-juelich.de

H. Poorter
Department of Biological Sciences, Macquarie University, North Ryde, Australia

Abbreviations

A	Water uptake rate per unit root length (ml h^{-1} m^{-1})
K_R	Local radial root conductance (cm^3 h^{-1} MPa^{-1})
K_{tot}	Total root conductance (cm^3 h^{-1} MPa^{-1})
L	Root length distribution (m)
$\hat{L}$	Normalized root length distribution
MRI	Magnetic resonance imaging
nMAE	Normalized mean absolute error

rSWF	Redistributive soil water flow (cm^3 cm^{-3} h^{-1})
RWU	Root water uptake rate (cm^3 cm^{-3} h^{-1})
SWaP	Soil water profiler
U_P	Plant-driven root water uptake distribution (cm^3 cm^{-3} h^{-1})
$\widehat{U}_P$	Normalized plant-driven root water uptake distribution
U_S	Soil-driven root water uptake redistribution (cm^3 cm^{-3} h^{-1})
U_{tot}	Total root water uptake rate (cm^3 h^{-1})
z_i	Depth of soil layer i (cm)
θ	Volumetric soil water content (cm^3 cm^{-3})
$\frac{\partial \theta}{\partial t}$	Soil water depletion rate (cm^3 cm^{-3} h^{-1})
Ψ_{collar}	Water potential at the plant collar (MPa)
Ψ_{soil}	Local soil water potential (MPa)
Ψ_{seq}	Equivalent, or plant sensed soil water potential (MPa)

Introduction

Spatial information on root water uptake rates is often required to describe soil–plant water relations. Since root water uptake profiles are challenging to measure, they are commonly approximated by the distribution of root length with depth, especially in macroscopic water uptake models (Coppola et al. 2015, 2019; Feddes et al. 2001; Wu et al. 1999). This approximation implies constant root water uptake rates per unit root length with depth. At the single root scale, however, uptake rates per unit root length vary with root branching order (Rewald et al. 2012), root type (Ahmed et al. 2016, 2018), distance from the root tip (Ahmed et al. 2016, 2018; Meunier et al. 2018; Steudle and Peterson 1998), root cortical senescence (Schneider et al. 2017) and root age (Schneider et al. 2020). Most of these parameters are related to root age, which is usually distributed along a vertical gradient, with older roots in shallow layers and younger roots in deeper layers (Koebernick et al. 2014). Therefore, one could expect a systematic variation in water uptake rates per unit root length with depth. Nevertheless, empirical studies, operating at a vertical resolution between 10 and 20 cm, generally suggest a good correlation between profiles of water uptake rates and root length (Ehlers et al. 1991; Sharp and Davies 1985; Shein and Pachepsky 1995), which supports the common assumption in macroscopic models. It needs to be

considered, however, that usually, a homogenous soil water potential distribution is a prerequisite for a reasonable comparison between root length distributions and water uptake profiles. This is highlighted by studies in which the strength of the correlation between root length and water uptake profiles varied among different soil water conditions (Dara et al. 2015; Sharp and Davies 1985; Shein and Pachepsky 1995). Since a homogeneous water potential distribution is difficult to achieve in experiments with natural soil substrates, approximating water uptake profiles by root length distributions still comes with uncertainty.

Generally local root water uptake rates (RWU) are determined by the radial root conductance (K_R) and the water potential gradient between soil (Ψ_{soil}) and the root xylem (Ψ_X). Focusing on the vertical axis with depth z, this writes:

$$RWU(z) = K_R(z) \cdot (\Psi_{soil}(z) - \Psi_X(z)) \tag{1}$$

In our study, we measure a component of the water uptake profile which is independent of Ψ_{soil}. This is achieved by measuring the short-term response of RWU to a change in light intensity which alters Ψ_X but not Ψ_{soil}, and thus, according to Eq. 1, only depends on K_R and Ψ_X. The theoretical framework for deriving a component of RWU which is independent of the soil water distribution has been developed by Couvreur et al. (2012). In their study, the authors show that local root water uptake rates (RWU) can be disentangled into two terms which we call plant-driven root water uptake distribution (U_P) and soil-driven root water uptake redistribution (U_S):

$$RWU(z) = U_P(z) + U_S(z) \tag{2}$$

$U_P(z)$ is determined by the spatial arrangement of root hydraulic conductance which depends on the distribution of intrinsic hydraulic conductivities and root length. $U_P(z)$ integrates to the total root water uptake rate (U_{tot}) across the whole root system. $U_S(z)$ additionally depends on the distribution of soil water potential (Ψ_{soil}) and can be interpreted as a redistributive water flow through the root system from relatively wet soil layers into relatively dry soil layers. Across the whole root system, $U_S(z)$ integrates to zero (Fig. 1A). Using the hydraulic network presented in Online Resource 1, we show in Appendix 1 that in a simplified form (compare Couvreur et al. (2012)), U_P and U_S can be expressed as:

Fig. 1 A Scheme of different water flow patterns in the soil root system, separated into vertically stacked layers. Local root water uptake rates (RWU) are the sum of the plant driven root water uptake distribution (U_P) and the soil driven root water uptake redistribution (U_S). U_P is the local fraction of the total root water uptake rate, determined by the local root conductance (K_R). Direct water flow from wetter to drier soil layers is called redistributive soil water flow (rSWF). **B** Overview of the measured parameters and the tested hypotheses. Normalized root water uptake profiles ($\hat{U}_P$) were determined with the SWaP, normalized root length profiles ($\hat{L}$) were determined with MRI. Based on these profiles we calculated the water uptake rates per unit root length (A) over depth. We tested the null hypothesis (H_0) that A is constant over depth, and the alternative hypothesis of systematic deviations of A with depth (H_1 or H_2)
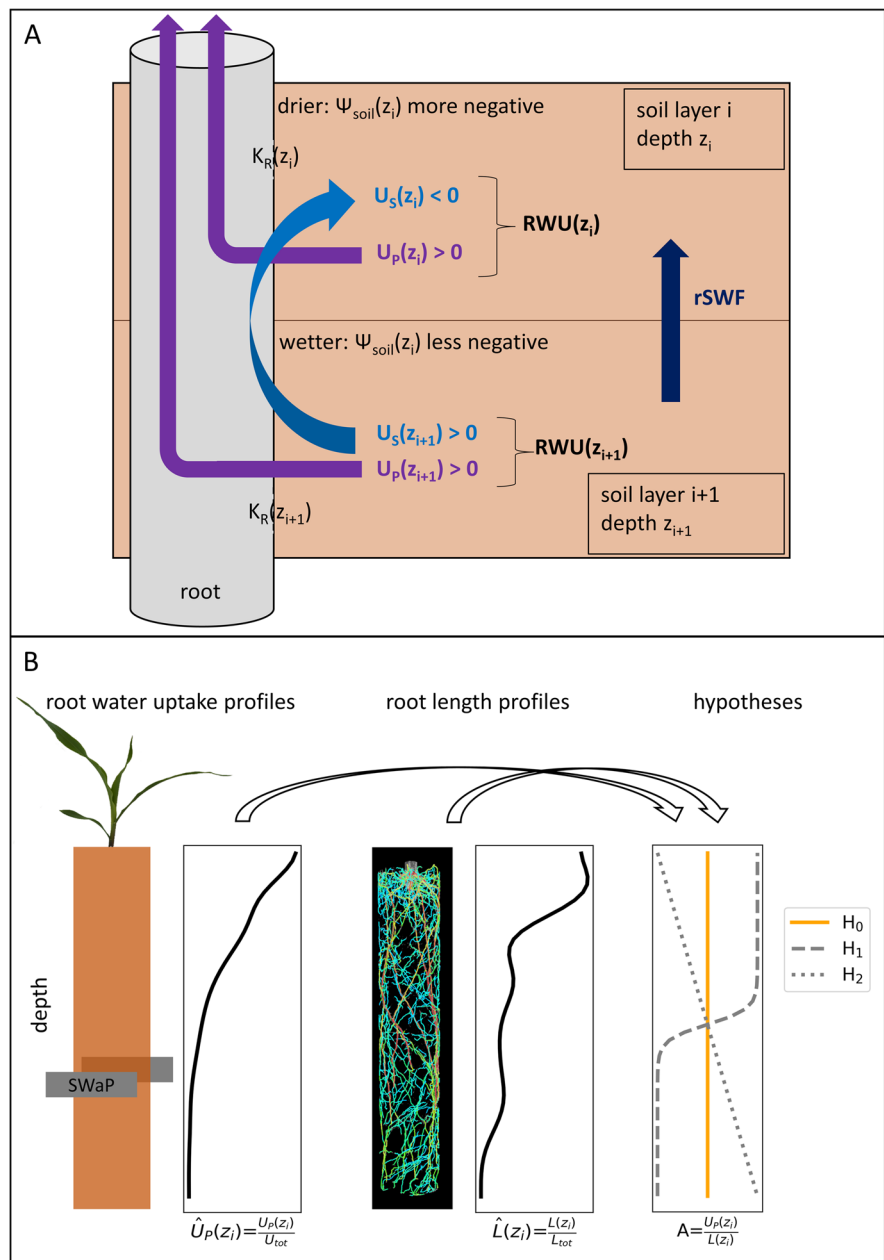
$$U_P(z) = U_{tot} \cdot \frac{K_R(z)}{K_{tot}} \text{ and } U_S(z) = K_R(z) \cdot (\Psi_{soil}(z) - \Psi_{seq})$$
(3)

In Eq. 3 we used the total water uptake rate (U_{tot}), the total root conductance (K_{tot}), and the plant sensed soil water potential (Ψ_{seq}). Note that K_{tot} and Ψ_{seq} are not measured in our study but are introduced here, to describe the meaning of U_P and U_S. In case of a homogeneous distribution of soil water potential ($\Psi_{soil}(z) = \Psi_{seq}$, in all layers), U_S becomes zero throughout. Therefore, U_P reflects the distribution of water uptake rates in a soil with uniform water potential distribution (corrected for gravity). Deviations from a uniform soil water distribution are considered by U_S.

Due to its independence of the soil water distribution, U_P is better suited than RWU to analyze how well water uptake profiles can be approximated by root length distribution. Recently, a method was introduced to measure U_P without actually depending on a uniform soil water distribution, using a highly precise soil water sensor in combination with a fluctuating light intensity (van Dusschoten et al. 2020). With this technology, we test the null hypothesis that root water uptake rates per unit root length (A) are constant with depth:

$$H_0 : A(z) = \frac{U_P(z)}{L(z)} = constant \qquad (4)$$

As alternative hypothesis, we test whether water uptake rates per root length vary systematically with depth, indicating a spatial gradient of root conductivity. Figure 1B gives an overview over the analyzed parameters and the tested hypotheses. Root system architecture potentially affects our hypothesis, since a simulation study predicted less variation in water uptake rates per root length for taproot compared to fibrous root systems (Javaux et al. 2013). We therefore tested whether H_0 is true across four different crop species: two monocots with a fibrous root system, barley and maize, and two dicots with a taproot system, zucchini, and faba bean. We performed the following analysis for each of the four species: In a first step, we analyzed to what extent the variation of U_P with depth is explained by a variation of L with depth and to what extent by a variation of A with depth. In a next step, we evaluated H_0 by testing for significant differences between water uptake rates per root length in shallow (upper third of the pots) and deeper layers (lower two thirds). Potential deviations from H_0 would indicate a variation of root conductivity. Since root conductivity is closely linked to root diameter (Ahmed et al. 2016; Frensch and Steudle 1989; Huang and Eissenstat 2000), we checked in a third step, whether variations of A(z) can be explained by root diameter distributions over depth.

Material and methods

Plant growing conditions

We grew four different plant species: the monocots barley (*Hordeum vulgare*), and maize (*Zea mays*), and the dicots faba bean (*Vicia faba*), and zucchini (*Cucurbita pepo cylindrica*). Seeds were germinated for 2–3 days in the dark on moistened germination paper. Seedlings were transferred into soil-filled PVC pipes (50 cm high, Inner Diameter: 8.1 cm), suitable for both MRI and SWaP measurements. We used a sandy loam, collected in Kaldenkirchen, Germany with 73.3% sand, 23.1% silt, 3.6% clay, (Pohlmeier et al. 2009) mixed with 20% (v) coarse sand (0.7–1.4 mm). Water saturation was reached at volumetric soil water content (θ) of 40.7%. The soil type was selected because it wets easily and uniformly within half a day after rewatering. Additionally, its water retention curve is relatively flat in the wet regime, making it easier to avoid large vertical soil water potential gradients. Note that even though our measurement of U_P is independent of the soil water potential distribution, vertical soil water flows would introduce noise during the analysis process. Furthermore, the soil type used leads to a good image quality of the MRI measurements which is related to the low silt, clay, and ferromagnetic content (Pflugfelder et al. 2017). The pots were filled with soil to a height of 45 cm, resulting in a total substrate volume of 2.32 l. Pots were filled under gentle shaking to promote uniform compaction, achieving a bulk density of 1.47 kg/l. Four plants per species were grown in the prepared pots in a climate chamber providing a controlled temperature of 21.5 °C ± 0.2 °C and a VPD_{air} of 1.49 kPa. Plants were watered from the top every 2nd or 3rd day to keep them well-watered at an average θ of above 20% (v/v). Before and during water uptake measurements, plants were not watered for approximately 24 h to minimize spatial gradients of soil water potential during the measurement, as confirmed by our measurements (Fig. 3). For fertilization, NPK nutrient salt (Hakaphos Red; Compo Expert; 8% N, 12% P, 24% K), diluted in water at 0.3% (v/v) was given to the plants once a week. The total amount of fertilized water supplied to the plants depended on the actual water use and varied between 30 ml (1st week) and up to 200 ml (4th week). We used a water-cooled LED panel (3200 K, 5×5 LEDs á 20 W) for illumination. During the day, two levels of light intensity alternated in periods of two hours for 14 h in total (three low light periods and four high light periods) for the full growing and measurement period. Photosynthetically active radiation of the lower level was 500 μmol m^{-2} s^{-1}, that of the higher level 1000 μmol m^{-2} s^{-1}. The light intensity

sums up to a daily light integral of 39.6 mol m^{-2} d^{-1}. This light fluctuation was required for the derivation of root water uptake profiles as described below. Twenty-eight days after germination, we measured the root water uptake profiles with the SWaP and the root length distribution with MRI of each individual plant. Within one day, we could measure all four replicates of one species. Below, we describe the SWaP and MRI measurements in detail.

SWaP measurement of $\widehat{U}_P(z_i)$

We measured $\widehat{U}_P$ with a recently developed soil water profiler (SWaP) (van Dusschoten et al. 2020). The sensors of the SWaP basically consist of two opposing copper plates (7×5 cm^2) in a 12 cm high PVC sleeve, shielded with aluminum. The sensors partially enclose the pots with soil columns and are movable along the z-axis. The copper plates form a capacitor which is connected to a coil, forming a resonator circuit. The resonance frequency of the circuit is a function of the electrical permittivity of the material in between the copper plates, which is largely determined by the soil water content θ. Thus, measuring the resonance frequency allows determination of θ as described below. A vector network analyzer (DG8SAQ, VNWA3, SDR-Kits, UK) was used to determine the resonance frequency of the circuit by applying a frequency sweep between 150 and 220 MHz. The sensors move vertically along the pots and measure the resonance frequency in equidistant steps of 1 cm. A complete scan of four pots with 45 cm high soil columns simultaneously took around 12 min. To synchronize with light fluctuations, scans were started every 15 min. For conversion of the resonance frequency into θ, we measured a calibration curve. To this end, we filled 12 cm high PVC pots with soil at a defined bulk density (1.47 kg/l, as used for plant growth) and a defined θ ranging from 2 to 30% and measured the resulting resonance frequency with the SWaP. The data were fitted using a second order polynomial (Online Resource 2). This procedure enabled us to measure the vertical θ profiles of our soil columns in 1-cm steps.

For our analysis, we interpreted the 45 cm high soil column as 45 stacked layers each of 1 cm height and uniform θ. The layers were indexed i=1 (top layer),..., 45 (bottom layer) with the top of each layer at depth $z_i=0$ cm,..., 44 cm. Given the 12 cm height of the

SWaP sensors, the measurement at each 1-cm layer is not the precise θ value in that layer, but a convolution of (1) the electrical field strength between the copper plates and (2) the 12 soil layers enclosed by the sensor. To achieve a spatial resolution of 1 cm, a deconvolution was applied. This procedure requires measuring the exact θ-values at the pot borders and the profile of the electrical field strength. Given these values we performed a numerical deconvolution. As this amplifies errors, we constrained the deconvoluted result by a regularization term which reduces fluctuations of the profile.

Given the deconvolved θ profiles over time we could, in a next step, derive the profiles of water uptake rates. For that, we calculated the rate of change in water content over time ($\frac{\partial\theta(z_i,t)}{\partial t}$) in each layer. A change in water content in layer i is caused by local RWU, redistributive soil water flow (rSWF) between adjacent layers, and evaporation in the top layer $E_s(t)$:

$$\frac{\partial\theta(z_i,t)}{\partial t} = \text{RWU}(z_i,t) + \text{rSWF}(z_i,t) + \begin{cases} E_s(t), z_i = 0 \\ 0, z_i \neq 0 \end{cases}$$
(5)

Using Eq. 2 we can express RWU as the sum of U_P and U_S with $U_P(z_i,t) = \frac{\widehat{U}_P(z_i) \cdot U_{tot}(t)}{V}$, total pot volume V and $U_{tot}(t) = \sum_{i=1}^{45} \frac{\partial\theta(z_i,t)}{\partial t}$. Neither U_S nor rSWF contribute to U_{tot} but sum up to zero across the whole pot. We summarize these two terms as soil water redistribution through soil and roots (S_r) and write Eq. 5 as:

$$\frac{\partial\theta(z_i,t)}{\partial t} = \widehat{U}_P(z_i) \cdot \frac{U_{tot}(t)}{V} + S_r(z_i,t) + \begin{cases} E_s(t), z_i = 0 \\ 0, z_i \neq 0 \end{cases}$$
(6)

To determine $\widehat{U}_P$ from Eq. 6, we make use of the light intensity fluctuating between a lower and a higher level at a period of two hours. The alternating light intensity induces a fast response of the transpiration rate, via stomatal regulation, and thus U_{tot}. Note that the transpiration rate and U_{tot} are almost similar, and only differ by the shoot growth rate. The response of U_P to a change of U_{tot} is much faster than the response of S_r, as it takes time to generate water potential gradients within the soil which drive both rSWF and Us. Therefore, U_P and S_r can be separated based on their response rate to fluctuating light intensity. Biologically, this can be understood as follows: A greater local root conductance leads to a greater

change in the water uptake rate when the light intensity changes. Therefore, the stronger the local $\frac{\partial \theta(t)}{\partial t}$ responds to a change in light intensity, and thus in U_{tot}, the greater the local root conductance, and thus U_P. Mathematically, $\widehat{U}_P$ can be derived as slope of a linear regression between $\frac{\partial \theta(t)}{\partial t}$ and $U_{tot}(t)$ according to Eq. 6 (Online resource 3). Such a regression was performed in each layer separately, using the data acquired during a 12 h period (7.00 am to 7.00 pm) covering three high and low light intensity periods of two hours each.

Determination of soil water potential and conductance

The soil water retention curve was measured using the evaporation method (Peters and Durner 2008) with the HYPROP setup (METER Group, Munich, Germany). The characteristic parameters of the water retention curve were obtained by fitting a Brooks-Corey model (Brooks and Corey 1964) to the measured data of the pressure head h (cm) for varying θ:

$$h(\theta) = \alpha^{-1} \left(\frac{\theta - \theta_r}{\theta_s - \theta_r} \right)^{-\frac{1}{\lambda}} \tag{7}$$

with saturated water content θ_s, residual water content θ_r, air entry pressure head α^{-1} (cm), and a dimensionless pore size index λ. To obtain the soil water potential Ψ_{soil}, a gravity component was added to the pressure head:

$$\Psi_{soil}(\theta(z)) = (h(\theta(z)) - z) \cdot 9.8 \cdot 10^{-5} \frac{MPa}{cm} \text{ with depth } z = 0 \text{ cm}, \dots, 44 \text{ cm}. \tag{8}$$

MRI measurement and processing of root length

Roots were non-invasively imaged using MRI. For logistical reasons, MRI measurements were either shortly before or after the SWaP measurements. Since plants were not under controlled conditions during MRI, scanning was preferably conducted during the night. The MRI setup consisted of a 4.7 T vertical wide bore (310 mm) magnet (Magnex, Oxford, UK) and a gradient coil (ID 205 mm (MR Solutions)) providing gradients up to 400 mT/m. The MRI experiments were controlled using an MR Solutions (Guildford, UK) console. NMRooting software (van Dusschoten et al. 2016) was used to analyze MRI data and calculate root length. Data of the root system were arranged in 45 vertical layers of 1 cm height (across a pot diameter of 8.1 cm). Using NMRooting, we obtained the root length present in each layer. For a similar MRI setup (van Dusschoten et al. 2016), a detection limit for root diameters between 200 μm and 300 μm was reported.

Harvest and root scanning

To include the fine root fraction below the detection limit of MRI, roots were harvested after the MRI or SWaP measurement respectively. Since we were interested in the vertical distribution of root traits, soil columns were taken out of the pots and cut into five blocks of 9 cm height each. The roots were isolated from the soil using sieves with different mesh sizes (0.3 mm to 2.0 mm) and stored in a solution of 70% water and 30% ethanol. Roots of each block were scanned separately. We used WinRHIZO software (Regent Instruments, Ottawa, Canada) to analyze total root length and root length in 20 equidistant diameter classes ranging from 0.0 mm to 2.0 mm (last class included all roots thicker than 2.0 mm) for all 5 blocks per plant separately. Using the distribution of harvested roots, we calculated correction factors for each 9 cm high soil block. The MRI measured root distribution was corrected accordingly. Finally, we applied the same convolution and deconvolution procedure to the root length profile as to $\widehat{U}_P$ to achieve a similar degree of smoothing caused by this procedure. Normalized, corrected, and deconvolved root length profile is called $\widehat{L}$. Leaf area and shoot fresh weight were also determined at harvest.

Quantitatively explaining the variation in UP(z)

Here we use a concept which has been developed to relate how important the variation of each of two factors of a product is to explain the variation of the product (Poorter and Nagel, 2000). For that we write U_P as product of L and A:

$$U_P = L \cdot A \qquad (9)$$

and apply an ln transformation:

$$ln(U_P) = ln(L \cdot A) \qquad (10)$$

which can be written as:

$$1 = \frac{ln(L)}{ln(U_P)} + \frac{ln(A)}{ln(U_P)} \qquad (11)$$

Given the U_P, L, and A profiles of a plant or species, each consisting of 45 values, we thus linearly fitted the ln of the 45 U_P values against the ln of the 45 L or A values respectively. Then the two terms on the right-hand side of Eq. 11 were determined as the slopes of the linear fits. According to Eq. 11, these two slopes add up to one, and are a measure for the relative importance of L, and A in explaining variation in U_P.

Results

Characteristic plant and soil parameters

Maize and zucchini had significantly greater shoot fresh weight than barley and faba bean (14–50 g) (Fig. 2). In barley, also the leaf area was significantly smaller than in maize and zucchini (199–576 cm^2). The total root length of faba bean (27 m) was significantly smaller than that of the other species (82–94 m). During the 12 h measurement period, zucchini took up significantly more water (95 ml) than
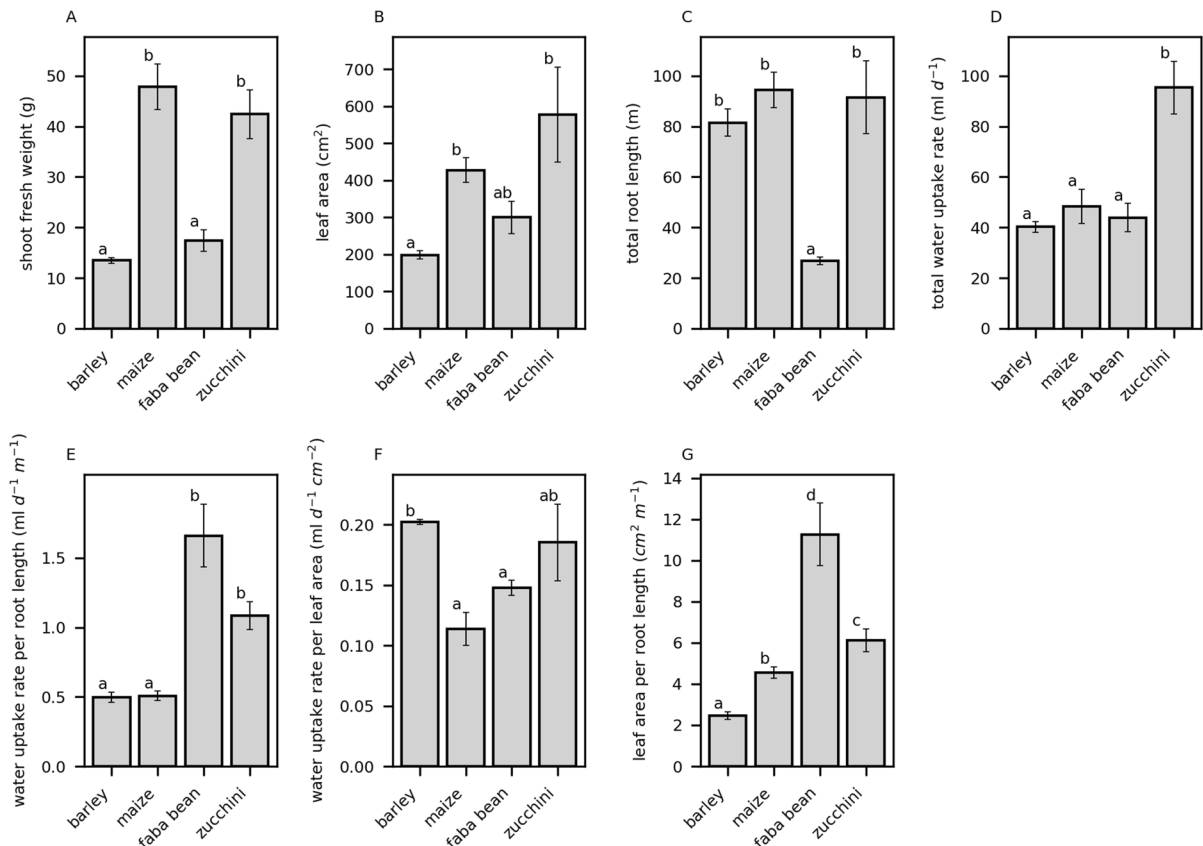
Fig. 2 Characteristic parameters of the species at the day of measurement: **A** shoot fresh weight, **B** leaf area, **C** total root length, **D** total root water uptake rate, **E** Water uptake rate per unit root length, **F** water uptake rate per leaf area, and **G** root-to-shoot ratio, expressed as leaf are per root length. Height of the bars are species averages ($n=4$), error bars are standard errors of the mean. Differences between species were considered significant if p-values of a Student's t-test were < 0.05. Significant differences between groups are indicated by different letters

the other species (40 – 48 ml). The total water uptake rate per unit length was significantly greater in faba bean (1.7 ml d^{-1} m^{-1}) and zucchini (1.1 ml d^{-1} m^{-1}) than in barley and maize (both 0.5 ml d^{-1} m^{-1}). However, water uptake per unit leaf area was significantly greater in barley (0.20 ml d^{-1} cm^{-2}) than in maize and faba bean (0.11 – 0.15 ml d^{-1} cm^{-2}). Shoot to root ratio, expressed as leaf area per root length, was significantly different among all species. It was lowest in barley, followed by maize and zucchini and highest in faba bean (2.5 – 11.3 cm^2 m^{-1}).

For all species, we generally measured a vertical gradient in Ψ_{soil} with more negative values at the top and less negative values at the bottom (Fig. 3). This gradient was more pronounced at the end compared to the start of the measurement. At start, the average Ψ_{soil} with depth ($\overline{\Psi}_{soil}$) was similar (-9 to -11 kPa) among the four species. At the end of the measurement, $\overline{\Psi}_{soil}$ for zucchini (-21 kPa) was significantly more negative than for barley (-12 kPa) and faba bean (-13 kPa). For maize (-14 kPa), $\overline{\Psi}_{soil}$ was not significantly different from the other species. Ψ_{soil} profiles of each individual plant are shown in Online Resource 4.

Root length distribution explains 61 – 71% of variation in water uptake profiles

Due to the higher abundance of roots in shallow soil layers, water uptake profiles and root length were both generally high in top layers and declined with depth (Fig. 4). In maize, both profiles dropped rather sharply within the top 10 cm but declined smoother in barley and faba bean. In zucchini, both profiles were generally flatter compared to the other species. In barley, maize, and faba bean, $\widehat{U}_P$ was consistently
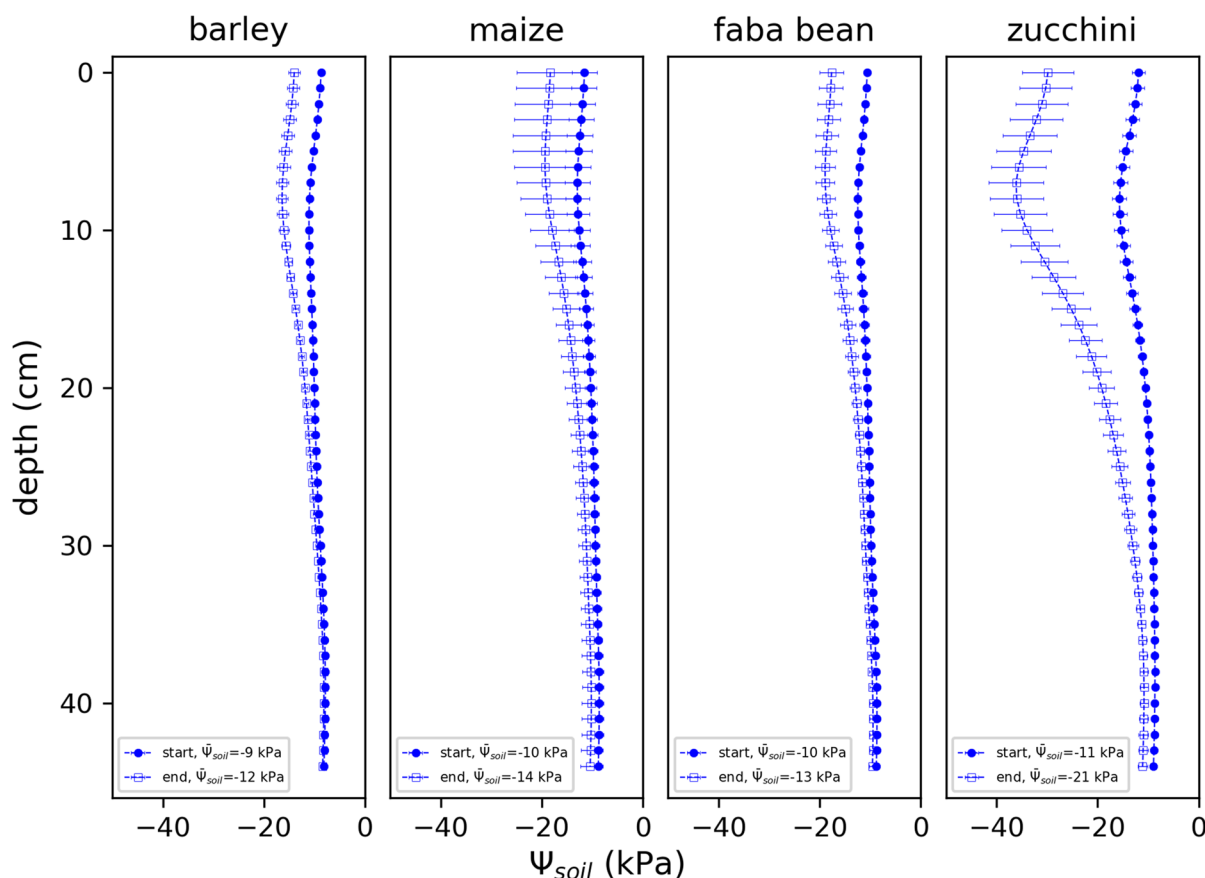
Fig. 3 Distribution of Ψ_{soil} at start (filled circles) and end (empty squares) of the SWaP measurements as species averages ($n=4$). Error bars are standard errors of the mean. Mean values over depth ($\overline{\Psi}_{soil}$) at start and end of the measurement are given in the legend

Fig. 4 $\hat{U}_P$ (blue) and $\hat{L}$ (red) as species averages ($n=4$). Horizontal error bars are standard errors of the mean in each layer. For total water uptake rate and total root length see Fig. 2
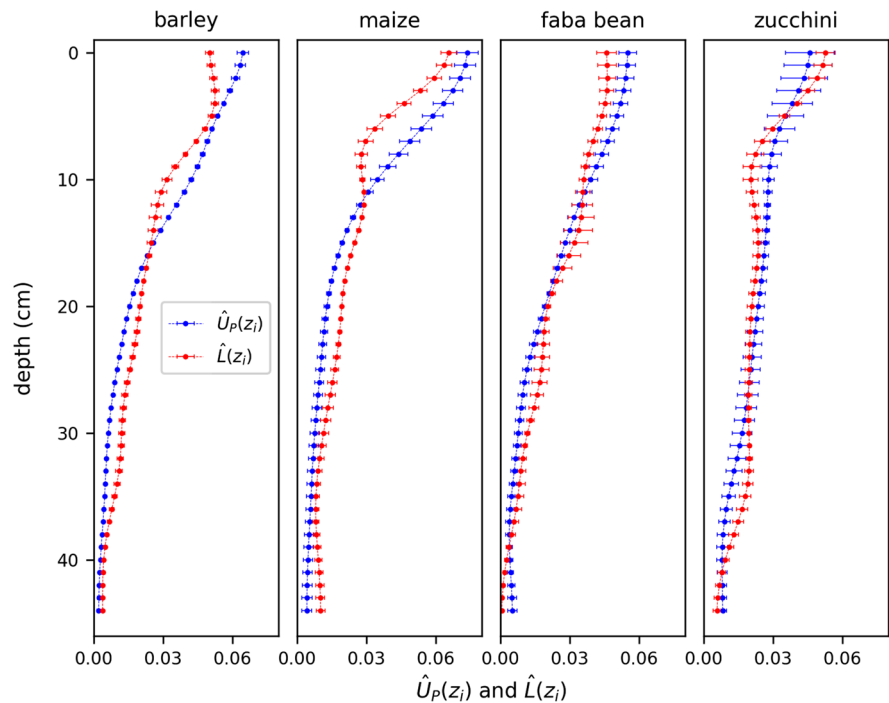
higher than $\hat{L}$ in the top layers but lower towards the bottom. $\hat{U}_P$ and $\hat{L}$ profiles of each individual plant are shown in Online resource 5. We evaluated to what extent variation in $U_P(z)$ is determined by variation in $L(z)$ and $A(z)$ respectively using Eqs. 9–11. This analysis was performed for each individual plant separately. Table 1 shows the results as species averages with standard errors of the mean. Between 61 and 71% of variation in $U_P(z)$ were explained by a variation in $L(z)$, 29–39% were explained by a variation in $A(z)$ without any significant differences among species.

Table 1 Relative importance of L and A in explaining variation in U_P with depth, determined as slopes of the linear fits between $\ln(L)$ and $\ln(U_P)$, and $\ln(A)$ and $\ln(U_P)$

	$\hat{L}$	$\hat{A}$
barley	0.70 ± 0.01	0.30 ± 0.01
maize	0.61 ± 0.08	0.39 ± 0.08
faba bean	0.71 ± 0.12	0.29 ± 0.12
zucchini	0.67 ± 0.14	0.33 ± 0.14

Values shown are mean values with standard error of the mean among the four replicates of each species. There were no significant differences between species as tested by a one-way ANOVA

Shallow roots show significantly greater uptake rates per unit length than deeper roots

The findings reported in Table 1 indicate a variation of water uptake rates per root length over depth, which implies deviations from our null hypothesis, H_0, of constant uptake rates per unit root length with depth. In a next step, we analyzed whether these deviations in $A(z)$ followed a spatial pattern (Fig. 5A). The vertical orange lines in Fig. 5A are the mean values over depth and represent H_0. In all four species, we observed that water uptake rates per root length in the top 15 cm (blue lines in Fig. 5A) were higher than in the bottom 30 cm (red lines), indicating a systematic deviation. Profiles of $A(z)$ of each individual plant are shown in Online resource 6. To quantify this trend of higher uptake rates per unit root length in top layers, we compared $A(z)$ between the top 15 cm and bottom 30 cm in each individual plant, and calculated the species averages (Fig. 5B). In barley, faba bean and maize, water uptake rates per root length were significantly higher in the top 15 cm compared to the bottom 30 cm. Except for one faba bean plant, this trend was found in each single plant (Online resource 6). In zucchini, there
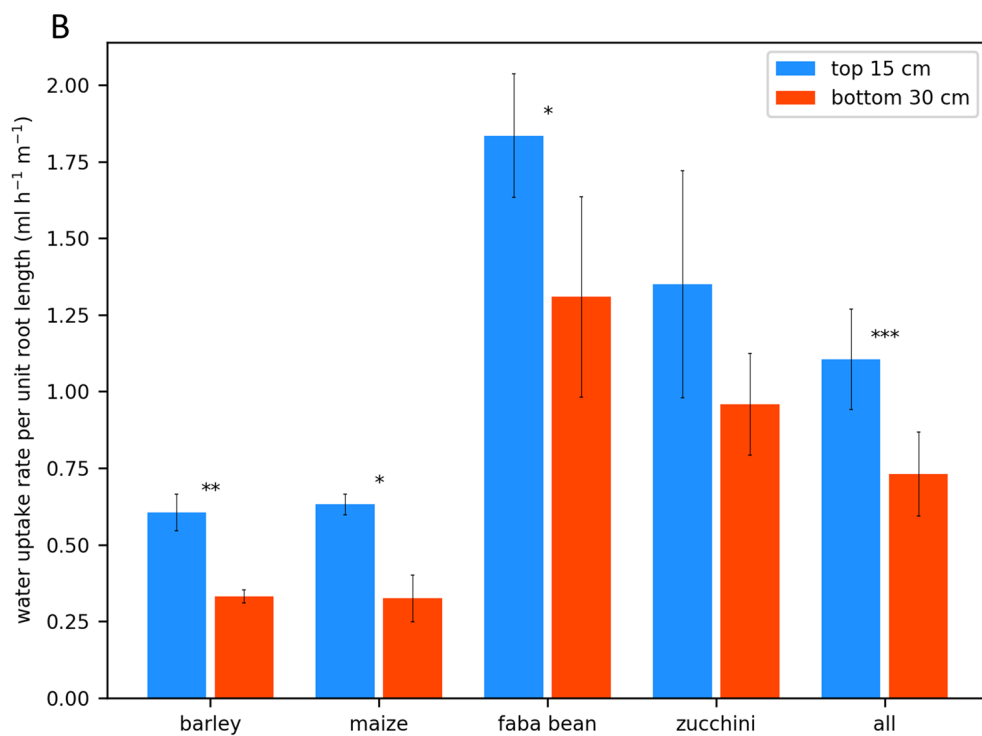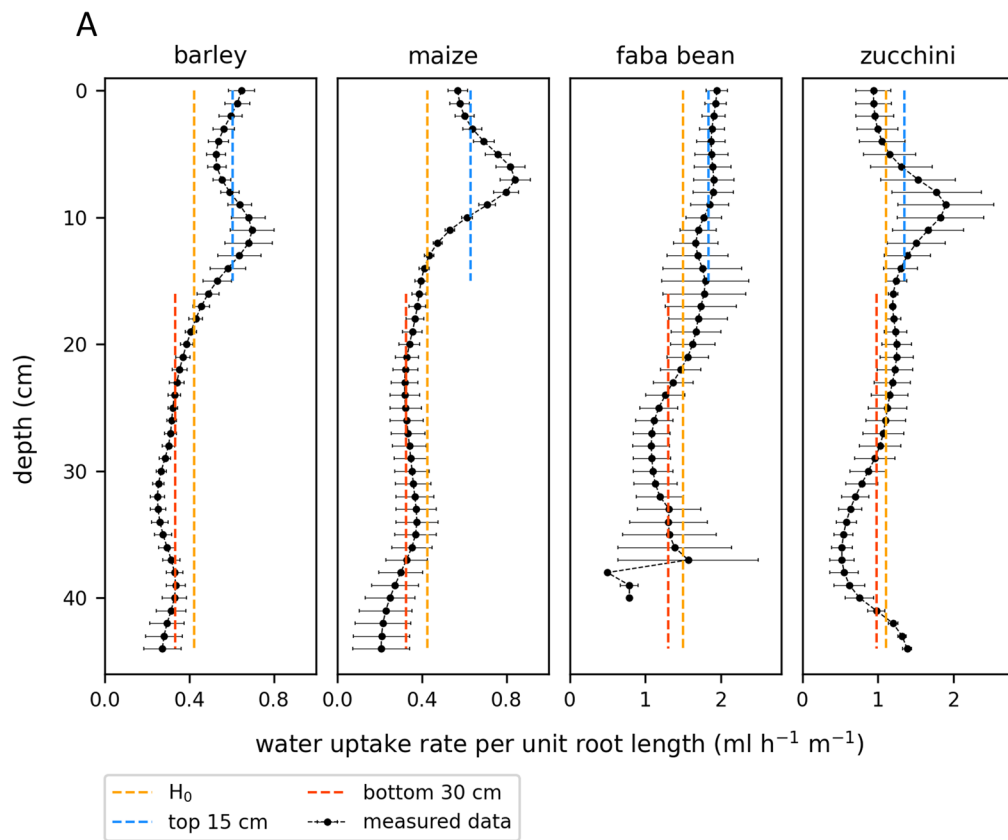
A Complete A(z) profiles. Colored vertical lines are mean values over depth ($n=4$) for the whole pot (orange), top 15 cm only (blue), bottom 30 cm only (red). Note that the orange line represents the null hypothesis of constant water uptake rates per unit root length. Data points are averages among species, error bars are standard errors of the mean. Layers with a root length below 10 cm caused considerable scatter of uptake rates per root length and thus were dropped for this and the following figure. This only concerned the bottom 5 cm of faba bean. **B** A(z) separated into the top 15 cm and bottom 30 cm of the pot. Height of the error bars are mean values among species ($n=4$), error bars are standard deviations of the mean. For each species, and all replicates we tested for significant differences between the top 15 cm and bottom 30 cm using a Student's t-test. Significant differences with a p-value below 0.05, 0.01, or 0.001 are indicated by *, **, or *** respectively

was no significant difference, and two individual plants had higher, two had lower uptake rates per length in top layers (Online resource 6). Among all 16 plants from the four different species, shallow roots had a significantly higher water uptake rate per root length than deeper roots (Fig. 5B).

Does the distribution of root diameter explain the variation of water uptake per root length?

The observed deviations from the null hypothesis indicate a vertical gradient in root conductivity with higher conductivity in shallow roots and lower conductivity in deeper roots. In a next step, we analyzed whether this pattern is reflected by the distribution of root traits (Fig. 6). Figure 6A exemplary shows an image of a root system from each species, acquired with MRI. Barley and maize have a fibrous root system with thicker (yellowish and reddish pseudo colors) seminal and nodal roots from which thinner (blueish pseudo colors) lateral roots emerge. In both species, the seminal and nodal roots were thinner in deeper layers compared to shallower layers. Faba bean and zucchini both have a taproot system with one main root growing vertically and lateral roots emerging from it. In faba bean, laterals in the upper soil layers appear as thick as the taproot. The laterals preferably grew horizontally and started spiraling downwards when they reached the pot borders. In zucchini, there was a clear trend of generally thicker roots in deeper layers compared to shallower layers for both, the main root and laterals. Note that the MRI had a detection limit between 200 μm and 300 μm. The color-coded diameter in Fig. 6A suggests that,

except for faba bean and deep layers of zucchini, a diameter of 0.5 mm is a reasonable threshold to distinguish between lateral roots and main roots. To quantify the distribution of laterals, we therefore analyzed the fraction of fine roots with a diameter below 0.5 mm over depth, using data from harvested and scanned roots (Fig. 6B). In barley, there was a continuous, significant decrease of this fine root fraction from 94% in the top soil layer to 69% in the bottom layer. In maize, the fine root fraction was greatest in the second layer (88% at a depth between 9 and 18 cm) and also decreased towards the bottom. In the deepest soil layer, it was significantly lower (66%) than in the second layer. In zucchini the decrease was even more pronounced, ranging from 92% in the top layer to only 30% in the bottom layer. Note, however that due to the general root thickening in the bottom layers of zucchini, a diameter-based distinction between laterals and main roots is difficult (Fig. 6A). In contrast to the other species, the fine root fraction in faba bean significantly increased from around 10% in the top 30 cm to 30% in the bottom layer. As mentioned above, the distinction based on root diameter in faba bean is questionable as laterals were comparably thick as the main root (Fig. 6A). Additionally, we analyzed the average root diameter over depth which revealed a similar picture (Online resource 7). For barley, maize and zucchini, the average diameter was almost constant in the top half of the pot and increased towards the bottom. Such a root thickening in deeper layers is typical for sandy soils (Lippold et al. 2021; Qin et al. 2005) and might be related to an increased ethylene concentration which reportedly induced root thickening in compacted soil layers (Pandey et al. 2021; Vanhees et al. 2022). For faba bean, however, average root diameter was lower in shallow than in deep soil layers.

Discussion

In the present study, we analyzed the common approximation of root water uptake profiles ($\widehat{U}_P$) by the distribution of root length ($\widehat{L}$) in 4 weeks old pot-grown crop plants. For that, we tested the hypothesis of a constant root water uptake rate per unit root length (A) with depth. We observed that only 61–71% of the variation in U_P with depth were explained by a variation of L with depth. 39–29% were explained
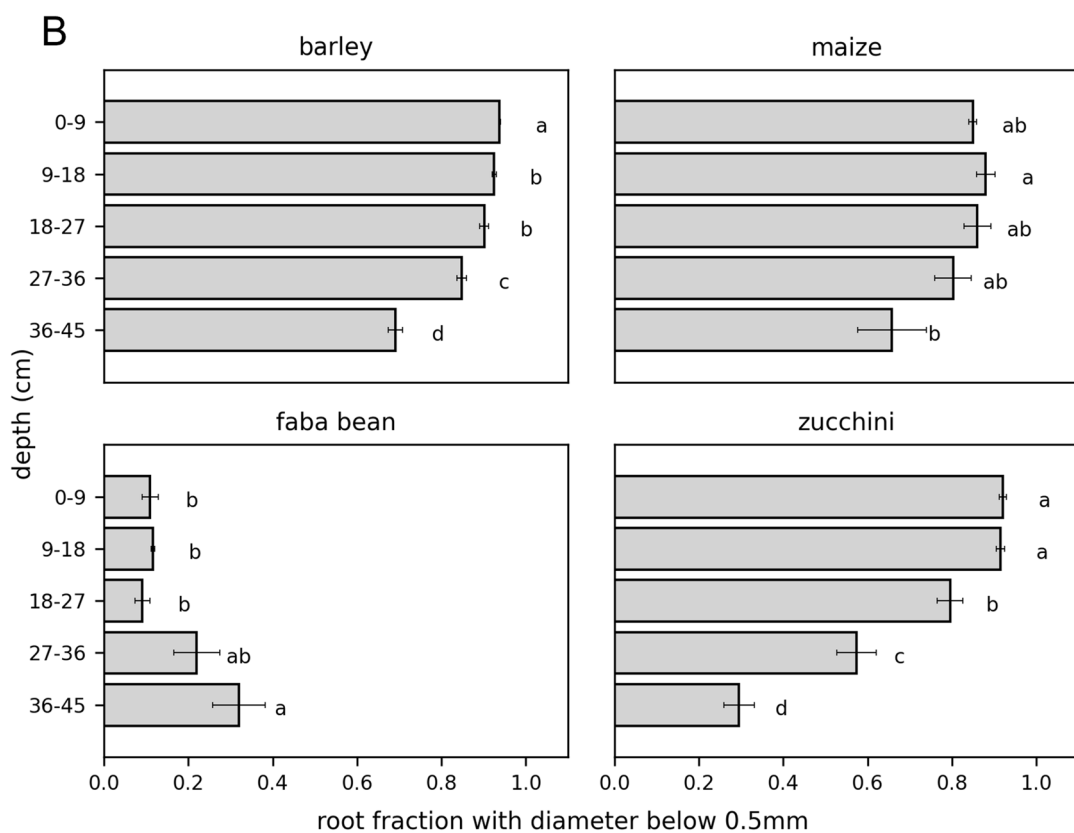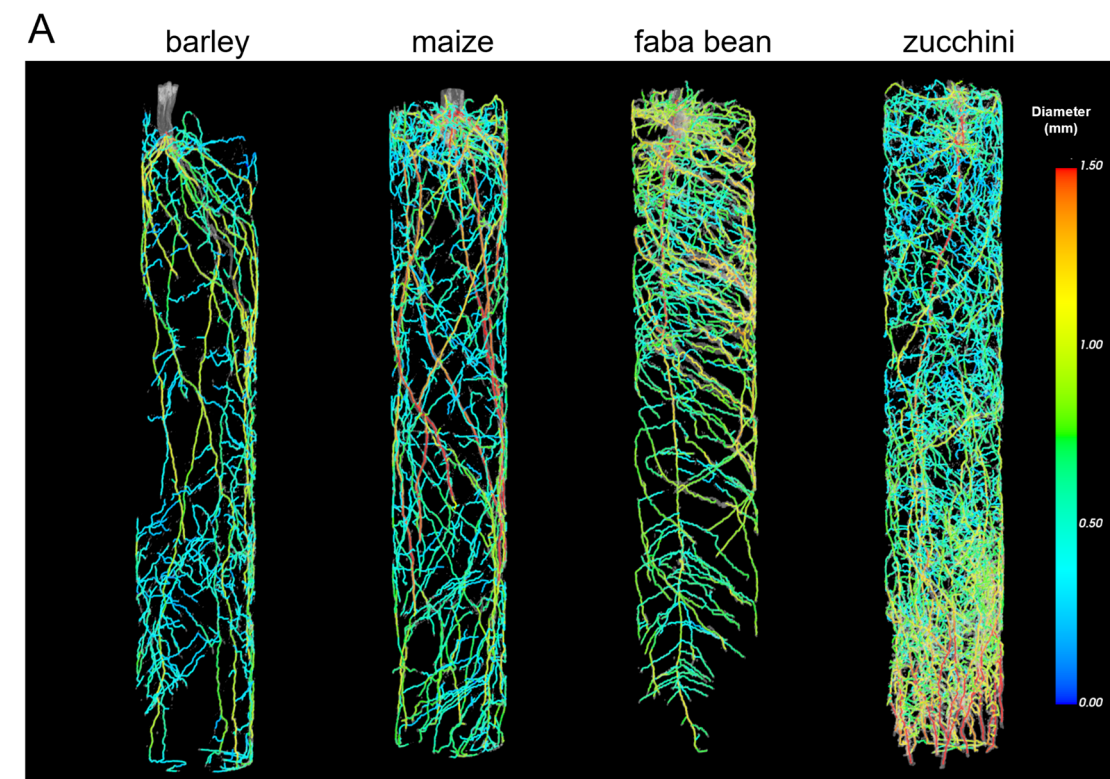
◄**Fig. 6** Distributions of characteristic root system traits measured with MRI and by scanning harvested roots. **A** Images of the different species' root systems and diameters acquired with MRI and analyzed with NMRooting. Exemplary, the image of one replicate per species is shown. Color code is root diameter ranging from blue (0 mm) to red (1.5 mm). Column size was 80.5 mm in diameter and 450 mm in height. **B** Fraction of fine roots with diameter below 0.5 mm over depth, derived by scanning of harvested roots. Horizontal bars are species averages, error bars are standard errors of the mean. Differences among depth were considered significant if p-values of a Student's t-test were < 0.05. Significant differences between different layers are indicated by different letters, starting with 'a' for the greatest value

by a variation in A with depth. The hypothesis of a constant A(z) did not hold as we found significantly greater water uptake rates per unit root length in the top 15 cm than in the bottom 30 cm of the pots in barley, maize and faba bean. Also in these three species, the fraction of lateral roots appeared to decrease towards the bottom.

Since spatial data on root hydraulic traits are rarely available, the approximation of root water uptake profiles by root length distributions was established in macroscopic water uptake models (Coppola et al. 2015, 2019; Feddes et al. 2001; Wu et al. 1999). Our data suggest that this approximation comes with limitations as only 61–71% (without significant differences between species) of variation in U_P could be explained by a variation in L (Table 1). These values are generally lower than those reported by the few quantitative, empirical studies on this topic (70–100% in oat and faba bean (Ehlers et al. 1991), 91–100% in oat and horse bean (Shein and Pachepsky 1995)). One major difference between these studies and our approach is that we measure a component of the root water uptake profile, namely $\widehat{U}_P$, which reflects the distribution of root hydraulic conductance and is independent of the soil water potential distribution. This was realized by measuring the fast response of local water depletion rates to a changing light intensity. The change in light intensity induces a change in the root xylem suction while the soil water potential at first stays constant. Therefore, how strong a change in xylem suction affects the local water depletion rate only depends on the distribution of root hydraulic conductance (see Eq. 1), and thus $\widehat{U}_P$. Typically, as in our measurements (Fig. 3), the soil water potential is lower (more negative) in upper layers than in deeper layers. This causes a redistributive water flow from

lower to upper soil layers through the roots. Therefore, U_S usually is in opposite direction to U_P in upper soil layers and in the same direction in deeper layers (Fig. 1A). According to Eq. 2 this results in RWU exceeding U_P in top layers and falling below it in bottom layers. Thus, if we had measured RWU instead of U_P the water uptake profiles (blue lines in Fig. 4) would have been closer to the root length profiles (red lines in Fig. 4). From this we conclude, that in studies measuring RWU instead of U_P, the predictive power of water uptake profiles by root length distributions is artificially increased by the impact of vertical soil water potential gradients on RWU. Approximating root water uptake profiles by root length distributions is equivalent to hypothesizing a constant water uptake rate per unit root length with depth. We observed that water uptake rates per root length were significantly greater in shallow roots compared to deeper roots (Fig. 5), emphasizing that the hypothesis does not hold. Two previous studies using neutron radiography to measure water fluxes into upper and lower parts of lupine root systems reported similar trends (Dara et al. 2015; Zarebanadkouki et al. 2013). Such a systematic deviation of water uptake rates per root length over depth is problematic for the common approximation of root water uptake profiles by root length distributions since it leads to a systematic underestimation of water uptake by roots in top layers and an overestimation in bottom layers. The trend of greater water uptake rates per root length in top layers was consistently observed for barley, maize and faba bean plants (Fig. 5 and Online resource 6). Note, that different physiological parameters, such as shoot size, root length, shoot–root ratio, and total water uptake rate per unit root length and leaf area (Fig. 2) varied, partly significantly, among these species. We therefore suggest that the trend of greater water uptake rates per root length in shallow roots is valid for a wider range of species and plants of different sizes and should be considered when water uptake profiles are approximated by root length distributions.

This leads us to the question of what caused the greater water uptake rates per root length in shallow roots. One potential reason is the impact of pot dimensions, which are known to constrain root growth (Poorter et al. 2012). However, since root length densities were greatest in shallow soil layers in our experiments (Figs. 4, 6A) we would also expect the strongest constrains in these layers. However,

water uptake rates per root length were greater in upper soil layers compared to deeper layers (Fig. 5). This emphasizes that potential consequences of constrained pot dimensions, such as saturation effects or limited root functioning, did not result in measurable impairment of water uptake rates.

Mathematically, local root water uptake rates are the product of the local radial root conductance and the water potential difference between the root xylem and the soil (Eq. 1). The radial root conductance depends on the radial root conductivity, an intrinsic hydraulic property, and root length. Therefore, uniform soil water potential distribution, uniform radial conductivity, and sufficiently high axial conductance to provide uniform water potentials in the root xylem are requirements for constant uptake rates per unit root length throughout the root system (Javaux et al. 2013). Given that U_P is independent of the soil water potential distribution, the difference in A(z) between shallow and deep roots must be caused by differences in the hydraulic parameters (i.e. radial root conductivity and xylem water potential) between the top and bottom part of the root system. As summarized by (Vetterlein and Doussan 2016), root radial conductivity depends on several root anatomical traits changing with root age, such as apoplastic barriers, cortex thickness, or aquaporin density. Towards the root tip, there usually is a lower degree of suberization (Huang and Eissenstat 2000; Steudle 1994; Steudle and Peterson 1998), thinner cell walls (McCormack et al. 2015; Steudle and Peterson 1998) and higher aquaporin expression (Gambetta et al. 2013), all of which results in a greater radial conductivity. This contributes to the generally high radial conductivity in lateral roots (Ahmed et al. 2016) or roots with a low branching order (Rewald et al. 2012). Our analysis suggests a greater fraction of fine lateral roots with a diameter below 0.5 mm in shallower than in deeper soil layers for barley, maize, and zucchini (Fig. 6B). If this fine root fraction indeed had a relatively high radial conductivity, it might have contributed to the greater water uptake rates per unit root length in shallow soil layers. However, as argued above, the anatomical features causing greater radial root conductivity usually appear towards the root tip. Therefore, we would expect a greater radial conductivity in deeper layers, where roots are generally younger (Koebernick et al. 2014). We can only speculate here, whether the effect of an increased root diameter, and thus, a

longer radial pathway outweighed the age-effect of a lower suberization and greater aquaporin expression in deeper roots. Note that for faba bean this quantitative analysis of root type distribution was not possible since lateral roots and main roots had a comparable diameter (Fig. 6A). Additionally, the general thickening of roots towards bottom layers (Online resource 7) could have obscured the distinction of lateral and main roots based on root diameter.

Another possibility is a less negative xylem water potential (less water suction) in deeper roots due to an insufficient axial conductance. The axial conductivity increases with increasing number and diameter of conducting xylem vessels. In addition, the axial conductance increases with increasing length of the hydraulic pathway (Frensch and Steudle 1989). In crops, both number and diameter of xylem vessels usually decrease towards the root tip, and thus with depth (Bramley et al. 2009; Clément et al. 2022; Frensch and Steudle 1989; Steudle and Peterson 1998; Watt et al. 2008). Note that in contrast, trees usually have a greater number and diameter of conducting root xylem in deeper layers (McElrone et al. 2004; Pate et al. 1995; Wang et al. 2015). For crops however, the root xylem anatomy, together with the long hydraulic pathway, lead to a decreasing axial conductance (Meunier et al. 2018; Zarebanadkouki et al. 2016), and finally to a less negative xylem water potential in deeper roots (Zarebanadkouki et al. 2016). In maize, the maturation of the late metaxylem in the main root was shown to occur around 25 cm from the root tip (Steudle and Peterson 1998) leading to increased axial conductance. This is spatially correlated to the rather sharp drop in A(z) that we observed within the top 15 cm in maize (Fig. 5A). In summary, the greater water uptake rates per unit root length in shallow roots in barley, maize and faba are most likely explained by a less restricted axial water transport as compared to deeper roots. This might be accompanied by the greater fraction of lateral roots, potentially leading to greater radial conductivity in shallow soil layers (Fig. 7).

In the field, greater water uptake efficiencies of shallow roots could be beneficial regarding the competition for rainwater in shallow soil layers. Our study, as well as those two studies reporting similar results (Dara et al. 2015; Zarebanadkouki et al. 2013), were performed with pot- or container-grown plants and, straightforwardly transferring the results

Fig. 7 Schematic evaluation of our hypothesis. Shallow roots generally have greater water uptake rates per unit root length (A(z)) than deeper roots. This is probably explained by a less negative xylem water potential in deeper layers due to an incomplete maturation of xylem vessels. Additionally, radial conductivity in shallow soil layers might be greater due to a higher fraction of fine lateral roots
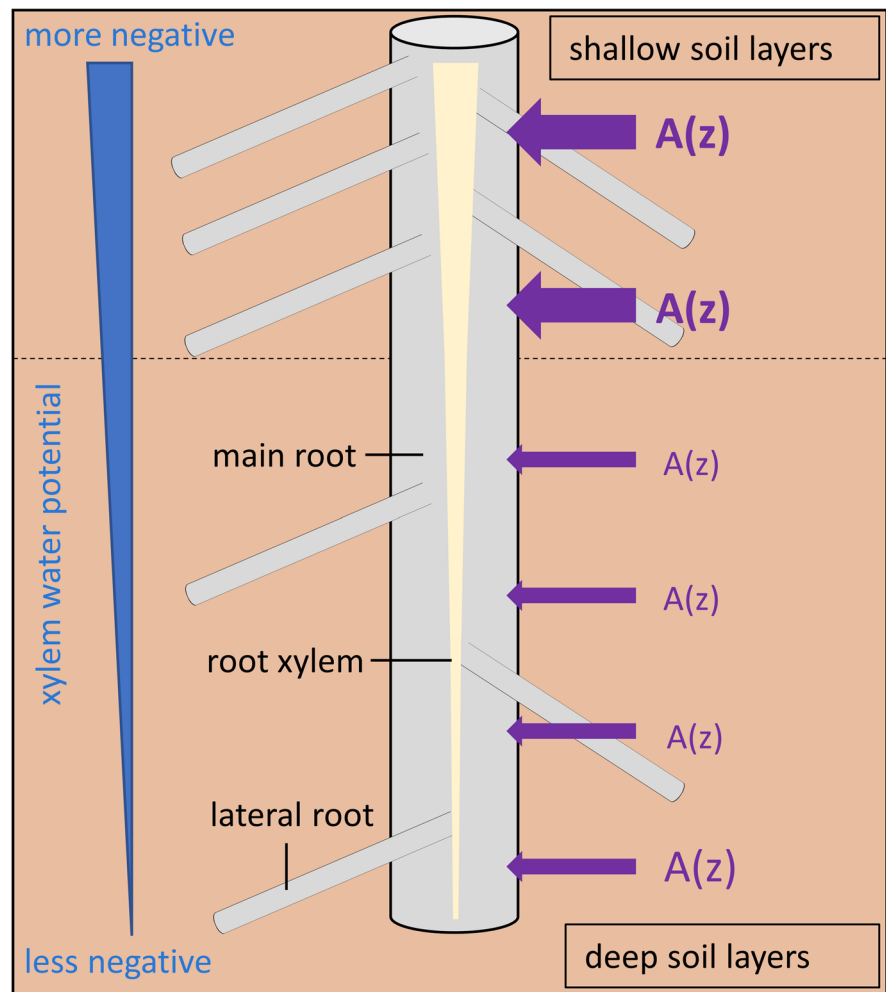
to field-grown plants is difficult. Only limited data on water uptake rates per root length from field experiments are available in the literature, probably because soil water conditions are barely controllable in the field, making a reliable measurement of water uptake profiles even more challenging. Two recent field studies in wheat suggest that root length and water uptake rates are asymptotically related due to a saturation of water uptake in upper soil layers with great root length densities (Gao et al. 2022; Zhang et al. 2020), which is opposite to our findings. It is possible that the restricted horizontal root growth in our pots led to a stronger vertical gradient in root system traits compared to field conditions, which might have contributed to the reduced uptake per root length in deeper layers. Further experiments are required to determine the distribution of

root hydraulic traits in field-grown plants, which is, however limited by the current technologies for measuring root water uptake patterns.

Concluding remarks

In the present study we tested the hypothesis of constant root water uptake rates per unit root length with depth to answer how reliably profiles of root water uptake rates can be approximated by root length distributions. We consistently found that in well-watered soil, water uptake rates per unit root length were significantly higher in shallower compared to deeper roots. Since this higher root activity in top soil layers was consistently observed among species which differed significantly in

various physiological parameters, it seems to be an universal trend. We suggest that it is explained by a limiting axial conductance of deeper roots. The greater uptake rates per unit root lengths of shallow roots need to be taken into account when water uptake profiles are used to estimate root length distribution or vice versa.

Data availability The data supporting the findings of this study are available from the corresponding author, Dagmar van Dusschoten, upon request.

Declarations

Appendix 1

In the following, we will derive how root water uptake profiles can be separated into one part, solely determined by root conductance (U_P), and a second one, additionally determined by the soil water potential distribution (U_S). For this purpose, we will use a simplified form of the model introduced by Couvreur et al. (2012), together with the following assumptions and considerations: The soil columns used in the experiments consist of 45 stacked, cylindrical layers of 1 cm height and 8.1 cm. Each layer is indicated by i with i $=$ 1,…, 45. The top of each layer is at depth z_i with $z_i = 0,…, 44$ cm. RWU(z_i) denotes the root water uptake rate, $K_R(z_i)$ the radial conductance, $K_X(z_i)$ the axial conductance, and $\Psi_X(z_i)$ the water potential in the xylem of the bulk roots in each layer. The water potential of the bulk soil in each layer is $\Psi_{soil}(z_i)$. The hydraulic network used for the analysis is presented in Online Resource 1.

With this, the root water uptake rate in each layer can be described as follows:

$$RWU(z_i) = K_R(z_i) \cdot (\Psi_{soil}(z_i) - \Psi_X(z_i)) \tag{1}$$

The total root water uptake rate (U_{tot}) is the sum of the root water uptake rates of all layers:

$$U_{tot} = \sum_i RWU(z_i) \tag{2}$$

U_{tot} can be expressed using the water potential at the plant collar (Ψ_{collar}), the total conductance between soil and plant collar (K_{tot}), and the equivalent soil water potential (Ψ_{seq}):

$$U_{tot} = K_{tot} \cdot (\Psi_{seq} - \Psi_{collar}) \tag{3}$$

Ψ_{seq}, as used in Eq. 14, reflects the overall soil water potential sensed by the plant. This parameter is obtained by weighing the soil water potential distribution by the distribution of root conductance (Couvreur et al. 2012). Solving Eq. 14 for Ψ_{collar} gives:

$$\Psi_{collar} = \Psi_{seq} - \frac{U_{tot}}{K_{tot}} \quad (4)$$

At this point, we assume that $K_X(z_i)$ is much higher than $K_R(z_i)$ and therefore $\Psi_X(z_i)$ is well approximated by Ψ_{collar}. Note that this assumption is not required for the separation of RWU in U_P and U_S as shown by Couvreur et al. (2012), but used here to keep the derivation concise. With this, Eq. 12 writes:

$$RWU(z_i) = K_R(z_i) \cdot (\Psi_{soil}(z_i) - \Psi_{collar}) \quad (5)$$

Using Eq. 15 to replace Ψ_{collar} in Eq. 16 gives after rewriting:

$$RWU(z_i) = K_R(z_i) \cdot \frac{U_{tot}}{K_{tot}} + K_R(z_i) \cdot (\Psi_{soil}(z_i) - \Psi_{seq}) \quad (6)$$

In Eq. 17, RWU is expressed as sum of two terms, of which the first one is independent of the soil water potential distribution.

We define $U_P(z_i) = K_R(z_i) \cdot \frac{U_{tot}}{K_{tot}}$ and $U_S(z_i) = K_R(z_i) \cdot (\Psi_{soil}(z_i) - \Psi_{seq})$, and write Eq. 17 as:

$$RWU(z_i) = U_P(z_i) + U_S(z_i) \quad (7)$$

Note that under the assumption $K_X(z_i) >> K_R(z_i)$, K_{tot} simplifies to the sum of the radial conductance of all layers: $K_{tot} = \sum_i K_R(z_i)$. Therefore, U_P can be normalized by division by U_{tot}:

$$\widehat{U}_P(z_i) = \frac{U_P}{U_{tot}} = \frac{K_R(z_i)}{K_{tot}} = \frac{K_R(z_i)}{\sum_i K_R(z_i)} \quad (8)$$

Without the assumption $K_X(z_i) >> K_R(z_i)$, $\widehat{U}_P(z_i)$ would additionally depend on the axial and radial conductance of other layers and thus on the overall root hydraulic architecture. Nevertheless, it would still be independent of $\Psi_{soil}(z_i)$.

References

Ahmed MA, Zarebanadkouki M, Kaestner A, Carminati A (2016) Measurements of water uptake of maize roots: the key function of lateral roots. Plant Soil 398(1–2):59–77. https://doi.org/10.1007/s11104-015-2639-6

Ahmed MA, Zarebanadkouki M, Meunier F, Javaux M, Kaestner A, Carminati A (2018) Root type matters: Measurement of water uptake by seminal, crown, and lateral roots in maize. J Exp Bot 69(5):1199–1206. https://doi.org/10.1093/jxb/erx439

Bramley H, Turner NC, Turner DW, Tyerman SD (2009) Roles of morphology, anatomy, and aquaporins in determining contrasting hydraulic behavior of roots. Plant Physiol 150(1):348–364. https://doi.org/10.1104/pp.108.134098

Brooks RH, Corey AT (1964) Hydraulic properties of porous media. Hydrol Pap 27(3):293–296

Coppola A, Chaali N, Dragonetti G, Lamaddalena N, Comegna A (2015) Root uptake under non-uniform root-zone salinity. Ecohydrology 8(7):1363–1379. https://doi.org/10.1002/eco.1594

Couvreur V, Vanderborght J, Javaux M (2012) A simple three-dimensional macroscopic root water uptake model based on the hydraulic architecture approach. Hydrol Earth Syst Sci 16(8):2957–2971. https://doi.org/10.5194/hess-16-2957-2012

Dara A, Moradi BA, Vontobel P, Oswald SE (2015) Mapping compensating root water uptake in heterogeneous soil conditions via neutron radiography. Plant Soil 397(1–2):273–287. https://doi.org/10.1007/s11104-015-2613-3

Ehlers W, Hamblin AP, Tennant D, van der Ploeg RR (1991) Root system parameters determinig water uptake of field crops. Irrig Sci 12:115–124. https://doi.org/10.1007/BF00192282

Feddes RA, Hoff H, Bruen M, Dawson TE, de Rosnay P, Dyrmeyer P, Jackson RB, Kabat P, Kleidon A, Lilly A, Milly PCD, Pitman A (2001) Modeling root water uptake in hydrological and climat models. Bull Amer Meteorol Soc 82(12):2797–2809. https://doi.org/10.1175/1520-0477(2001)082<2797:MRWUIH>2.3.CO;2

Gambetta GA, Fei J, Rost TL, Knipfer T, Matthews MA, Shackel KA, Andrew Walker M, McElrone AJ (2013) Water uptake along the length of grapevine fine roots: Developmental anatomy, tissue-specific aquaporin expression, and pathways of water transport. Plant Physiol 163(3):1254–1265. https://doi.org/10.1104/pp.113.221283

Huang B, Eissenstat DM (2000) Linking hydraulic conductivity to anatomy in plants that vary in specific root length. J Am Soc Hortic Sci 125(2):260–264. https://doi.org/10.21273/JASHS.125.2.260

Lippold E, Phalempin M, Schlüter S, Vetterlein D (2021) Does the lack of root hairs alter root system architecture of Zea mays? Plant Soil 467(1–2):267–286. https://doi.org/10.1007/s11104-021-05084-8

McCormack ML, Dickie IA, Eissenstat DM, Fahey TJ, Fernandez CW, Guo D, Helmisaari HS, Hobbie EA, Iversen CM, Jackson RB, Leppälammi-Kujansuu J, Norby RJ, Phillips RP, Pregitzer KS, Pritchard SG, Rewald B, Zadworny M (2015) Redefining fine roots improves understanding of below-ground contributions to terrestrial biosphere processes. New Phytol 207(3):505–518. https://doi.org/10.1111/nph.13363

McElrone AJ, Pockman WT, Martínez-Vilalta J, Jackson RB (2004) Variation in xylem structure and function in stems and roots of trees to 20 m depth. New Phytol 163(3):507–517. https://doi.org/10.1111/j.1469-8137.2004.01127.x

Pandey BK, Huang G, Bhosale R, Hartman S, Sturrock CJ, Jose L, Martin OC, Karady M, Voesenek LACJ, Ljung K, Lynch JP, Brown KM, Whalley WR, Mooney SJ, Zhang D, Bennett MJ (2021) Plant roots sense soil compaction through restricted ethylene diffusion. Science

371(6526):276–280. https://doi.org/10.1126/science.abf3013

Pate JS, Jeschke WD, Aylward MJ (1995) Hydraulic architecture and xylem structure of the dimorphic root systems of south-west australian species of proteaceae. J Exp Bot 46(8):907–915. https://doi.org/10.1093/jxb/46.8.907

Peters A, Durner W (2008) Simplified evaporation method for determining soil hydraulic properties. J Hydrol 356:147–162. https://doi.org/10.1016/j.jhydrol.2008.04.016

Pflugfelder D, Metzner R, Dusschoten D, Reichel R, Jahnke S, Koller R (2017) Non-invasive imaging of plant roots in different soils using magnetic resonance imaging (MRI). Plant Methods 13(1):1–9. https://doi.org/10.1186/s13007-017-0252-9

Pohlmeier A, Haber-Pohlmeier S, Stapf S (2009) A fast field cycling nuclear magnetic resonance relaxometry study of natural soils. Vadose Zone J 8(3):735–742. https://doi.org/10.2136/vzj2008.0030

Poorter H, Nagel O (2000) The role of biomass allocation in the growth response of plants to different levels of light, CO2, nutrients and water: A quantitative review. Funct Plant Biol 27(6):595–607. https://doi.org/10.1071/pp99173_co

Poorter H, Bühler J, Van Dusschoten D, Climent J, Postma JA (2012) Pot size matters: A meta-analysis of the effects of rooting volume on plant growth. Funct Plant Biol 39(11):839–850. https://doi.org/10.1071/FP12049

Qin R, Stamp P, Richner W (2005) Impact of tillage and banded starter fertilizer on maize root growth in the top 25 centimeters of the soil. Agron J 97(3):674–683. https://doi.org/10.2134/agronj2004.0059

Rewald B, Raveh E, Gendler T, Ephrath JE, Rachmilevitch S (2012) Phenotypic plasticity and water flux rates of Citrus root orders under salinity. J Exp Bot 63(7):2717–2727. https://doi.org/10.1093/jxb/err457

Schneider HM, Wojciechowski T, Postma JA, Brown KM, Lücke A, Zeisler V, Schreiber L, Lynch JP (2017) Root cortical senescence decreases root respiration, nutrient content and radial water and nutrient transport in barley. Plant, Cell Environ 40(8):1392–1408. https://doi.org/10.1111/pce.12933

Schneider HM, Postma JA, Kochs J, Pflugfelder D, Lynch JP, van Dusschoten D (2020) Spatio-temporal variation in water uptake in seminal and nodal root systems of barley plants grown in soil. Front Plant Sci 11(August):1–13. https://doi.org/10.3389/fpls.2020.01247

Sharp RE, Davies WJ (1985) Root growth and water uptake by maize plants in drying soil. J Exp Bot 36(9):1441–1456. https://doi.org/10.1093/jxb/36.9.1441

Shein EV, Pachepsky YA (1995) Influence of root density on the critical soil water potential. Plant Soil 171(2):351–357. https://doi.org/10.1007/BF00010291

Steudle E (1994) Water transport across roots. Plant Soil 167(1):79–90. https://doi.org/10.1007/BF01587602

Steudle E, Peterson CA (1998) How does water get through roots? J Exp Bot 49(322):775–788. https://doi.org/10.1093/jexbot/49.322.775

van Dusschoten D, Kochs J, Kuppe CW, Sydoruk VA, Couvreur V, Pflugfelder D, Postma JA (2020) Spatially resolved root water uptake determination using a precise soil water sensor. Plant Physiol 184(3):1221–1235. https://doi.org/10.1104/pp.20.00488

Vanhees DJ, Schneider HM, Sidhu JS, Loades KW, Bengough AG, Bennett MJ, Pandey BK, Brown KM, Mooney SJ, Lynch JP (2022) Soil penetration by maize roots is negatively related to ethylene-induced thickening. Plant, Cell Environ 45(3):789–804. https://doi.org/10.1111/pce.14175

Vetterlein D, Doussan C (2016) Root age distribution: how does it matter in plant processes? A focus on water uptake. Plant Soil 407(1–2):145–160. https://doi.org/10.1007/s11104-016-2849-6

Wang Y, Dong X, Wang H, Wang Z, Gu J (2015) Root tip morphology, anatomy, chemistry and potential hydraulic conductivity vary with soil depth in three temperate hardwood species. Tree Physiol 36(1):99–108. https://doi.org/10.1093/treephys/tpv094

Watt M, Magee LJ, McCully ME (2008) Types, structure and potential for axial water flow in the deepest roots of field-grown cereals. New Phytol 178(3):690. https://doi.org/10.1111/j.1469-8137.2008.02434.x

Wu J, Zhang R, Gui S (1999) Modeling soil water movement with water uptake by roots. Plant Soil 215(1):7–17. https://doi.org/10.1023/A:1004702807951

Zarebanadkouki M, Kim YX, Carminati A (2013) Where do roots take up water? Neutron radiography of water flow into the roots of transpiring plants growing in soil. New Phytol 199(4):1034–1044. https://doi.org/10.1111/nph.12330

Zarebanadkouki M, Meunier F, Couvreur V, Cesar J, Javaux M, Carminati A (2016) Estimation of the hydraulic conductivities of lupine roots by inverse modelling of high-resolution measurements of root water uptake. Ann Bot 118(4):853–864. https://doi.org/10.1093/aob/mcw154

Zhang XX, Whalley PA, Ashton RW, Evans J, Hawkesford MJ, Griffiths S, Huang ZD, Zhou H, Mooney SJ, Whalley WR (2020) A comparison between water uptake and root length density in winter wheat: effects of root density and rhizosphere properties. Plant Soil 451(1–2):345–356. https://doi.org/10.1007/s11104-020-04530-3

Clément C, Schneider HM, Dresbøll DB, Lynch JP, Thorup-Kristensen K (2022) Root and xylem anatomy varies with root length, root order, soil depth and environment in intermediate wheatgrass (Kernza®) and alfalfa. Ann Bot 1–16. https://doi.org/10.1093/aob/mcac058

Coppola A, Dragonetti G, Sengouga A, Lamaddalena N, Comegna A, Basile A, Noviello N, Nardella L (2019) Identifying optimal irrigation water needs at district scale by using a physically based agro-hydrological model. Water (Switzerland) 11(4). https://doi.org/10.3390/w11040841

Frensch J, Steudle E (1989) Axial and radial hydraulic resistance to roots of maize (Zea mays L.). Plant Physiol 91(2):719–726. https://doi.org/10.1104/pp.91.2.719

Gao Y, Chen J, Wang G, Liu Z, Sun W, Zhang Y, Zhang X (2022) Different responses in root water uptake of summer maize to planting density and nitrogen fertilization. Front Plant Sci 13(June). https://doi.org/10.3389/fpls.2022.918043

Javaux M, Couvreur V, Vanderborght J, Vereecken H (2013) Root water uptake: from three-dimensional biophysical processes to macroscopic modeling approaches. Vadose Zone J 12(4):vzj2013.02.0042. https://doi.org/10.2136/vzj2013.02.0042

Koebernick N, Weller U, Huber K, Schlüter S, Vogel H, Jahn R, Vereecken H, Vetterlein D (2014) In situ visualization and quantiication of three- dimensional root system architecture and growth using x-ray computed tomography. Vadose Zone J 13(8). https://doi.org/10.2136/vzj2014.03.0024

Meunier F, Zarebanadkouki M, Ahmed MA, Carminati A, Couvreur V, Javaux M (2018) Hydraulic conductivity of soil-grown lupine and maize unbranched roots and maize root-shoot junctions. J Plant Physiol 227(December 2017):31–44. https://doi.org/10.1016/j.jplph.2017.12.019

van Dusschoten D, Metzner R, Kochs J, Postma JA, Pflugfelder D, Buehler J, Schurr U, Jahnke S (2016) Quantitative 3D analysis of plant roots growing in soil using magnetic resonance imaging. Plant Physiol 170(March):01388.2015. https://doi.org/10.1104/pp.15.01388

Publisher's note Springer Nature remains neutral with regard to jurisdictional claims in published maps and institutional affiliations.